Biased diffusion in percolation systems: indication of multifractal behaviour

1987 J. Phys. A: Math. Gen. 20 L865

(http://iopscience.iop.org/0305-4470/20/13/010)

J. Phys. A: Math. Gen. **20** (1987) L865-L871. Printed in the UK

LETTER TO THE EDITOR

Biased diffusion in percolation systems: indication of multifractal behaviour

Armin Bunde†, Harald Harder†, Shlomo Havlin†‡ and H Eduardo Roman†

† Fakultät für Physik, Universität Konstanz, D-7750 Konstanz, Federal Republic of Germany

‡ Department of Physics, Bar-Ilan University, Ramat-Gan, Israel

Received 18 June 1987

Abstract. We study diffusion in percolation systems at criticality in the presence of a constant bias field E. Using the exact enumeration method we show that the mean displacement of a random walker varies as $\langle r(t)\rangle \sim \log t/A(E)$ where $A(E)=\ln[(1+E)/(1-E)]$ for small E. More generally, diffusion on a given configuration is characterised by the probability $P(r, t)$ that the random walker is on site r at time t. We find that the corresponding configurational average shows simple scaling behaviour and is described by a single exponent. In contrast, our numerical results indicate that the averaged moments $\langle P^q(t)\rangle = \langle \Sigma_r P^q(r, t)\rangle$ are described by an infinite hierarchy of exponents. For zero bias field, however, all moments are determined by a single gap exponent.

In recent years the problem of diffusion in disordered structures under the influence of an external bias field E has received much interest [1-13]. While some understanding has been achieved in the case of a topological bias [11-13], the situation for the more conventional 'Euclidean' bias is rather unclear (see in particular [6, 9, 10]).

In this letter we study in detail both types of biased diffusion on the infinite percolation cluster at criticality [14]. Using the exact enumeration method [15, 16] we present results for the mean displacements as well as for the average distribution functions and their fluctuations. In both cases we find that the mean displacements are proportional to $(\log t)^{\alpha}$ where α is close to unity and is independent of the field. The prefactor is proportional to $1/\{\ln[(1+E)/(1-E)]\}$ for small bias field E. More generally, for each random configuration the dynamics is completely characterised by the probability $P(r, t)$ that a random walker is on site r at time t when starting from the origin at $t=0$. We find that in both types of bias fields the configurational averaged distribution functions scale and can be described by a single exponent. In contrast, to characterise the (configurational averaged) moments of $P(r, t)$ our numerical results suggest an infinite hierarchy of exponents. Similar 'multifractal' behaviour has been observed recently in several physical systems [17-24]. For zero bias field, however, a single exponent is sufficient to characterise all moments.

Consider a random walker on the incipient infinite percolation cluster under the influence of a bias field. The bias field is modelled by giving the random walker a higher probability W_+ to move along the direction of the field and a lower probability W_- to move against the field,

$$W_{\pm} = a(1 \pm E) \tag{1}$$

0305-4470/87/130865+07$02.50

where $0 \leqslant E \leqslant 1$ is the strength of the field and a is an appropriate normalisation factor. The field can be either uniform in the xy direction ('Euclidean' bias) or directed in topological space [11-13] ('topological' bias), see figure 1. In a topological bias, every bond experiences a bias field which drives the walker away in chemical distance [25] (path length) from a point source. Consequently, the random walker has an enhanced probability W_+ to increase the chemical distance from the source in the next step, and a decreased probability W_- to decrease the chemical distance.

Diffusion in the presence of a topological bias field is conveniently described [11-13] by the mean chemical distance $\langle l(t)\rangle$ travelled by the walker up to time t, while for the Euclidean bias $\langle \boldsymbol{r}(t)\rangle$ is the appropriate quantity. By definition

$$\langle l(t)\rangle = \left\langle \sum_{\boldsymbol{r}} l(\boldsymbol{r}) P(\boldsymbol{r}, t) \right\rangle \tag{2a}$$

and

$$\langle \boldsymbol{r}(t)\rangle = \left\langle \sum_{\boldsymbol{r}} \boldsymbol{r} P(\boldsymbol{r}, t) \right\rangle \tag{2b}$$

where $l(\boldsymbol{r})$ is the chemical distance [25] of site $\boldsymbol{r}$ from the origin. The mean chemical distance in the case of a topological bias field has been studied before [11-13]. It was found [12] that in percolation at criticality (in $d = 2$ and in the Cayley tree)

$$\langle l(t)\rangle \sim \ln t / A(E) \tag{3a}$$

where $A(E) = \ln[(1+E)/(1-E)]$. To calculate $\langle \boldsymbol{r}(t)\rangle$ for the Euclidean bias we have used the exact enumeration method which enables us to enumerate $P(\boldsymbol{r}, t)$ exactly for each configuration. Our results for several values of E are shown in figure 2. They suggest also

$$\langle \boldsymbol{r}(t)\rangle \sim (\log t)^{\alpha} / B(E) \tag{3b}$$

where $B(E) = A(E)$ for small E and the exponent α is close to 1. From our data we cannot exclude the case $\alpha = d_l / d_f \simeq 0.88$, where $d_l \simeq \frac{5}{3}$ and $d_f = \frac{91}{48}$ are the topological and fractal dimensions, respectively. The relation $\alpha = d_l / d_f$ would mean that both topological and Euclidean bias are in the same universality class. In both cases, the

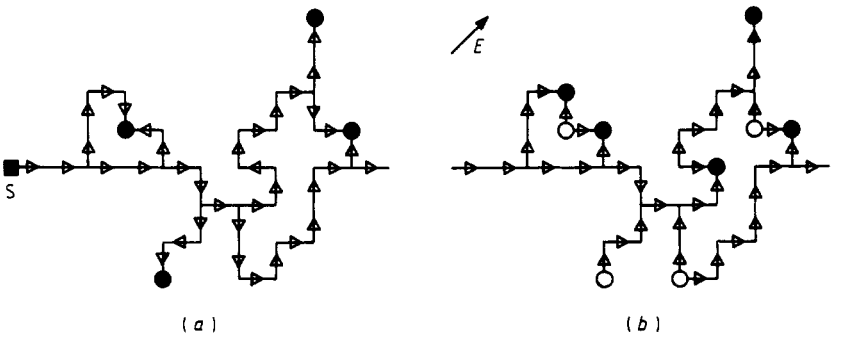

Figure 1. Illustrations of Euclidean bias (a) and the topological bias (b). The arrows represent the directions of the bias field along the bonds. S is the source of the topological field. The full circles denote those sites which are favourably occupied by a random walker ('hot sites') while the open circles represent those sites which the walker favours to leave ('cold sites').

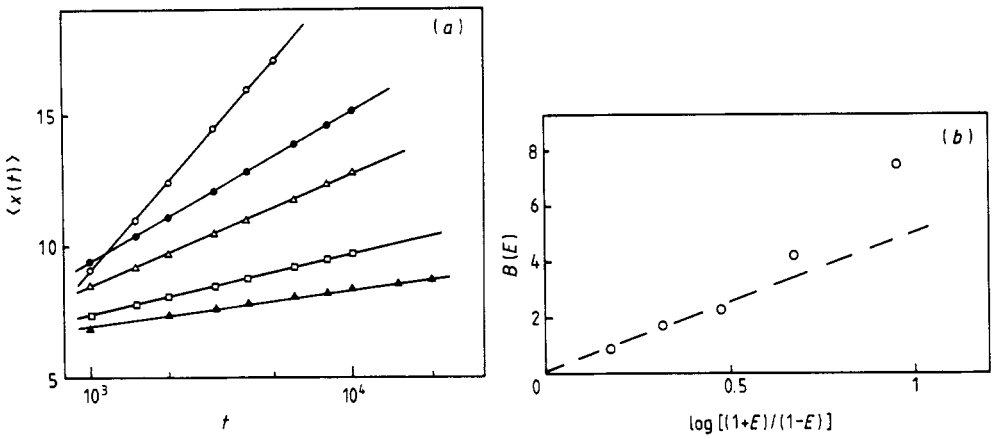

Figure 2. (*a*) Mean displacement $\langle x(t)\rangle$ against ln t for several Euclidean bias fields: $E = 0.2$ (○), 0.35 (●), 0.5 (△), 0.65 (□), 0.8 (▲). The results were obtained using the exact enumeration method and averages were taken over more than a hundred cluster configurations each. Due to symmetry $\langle y(t)\rangle$ is equal to $\langle x(t)\rangle$, which we also confirmed numerically. (*b*) Slopes $B(E)$ obtained from (*a*). The broken line shows $A(E) = \ln[(1+E)/(1-E)]$.

origin of the logarithmic slow motion lies in the fact that the walker can easily get stuck in dangling ends and loops ('hot' sites, see figure 1) which exist in all length scales at criticality.

In order to obtain a deeper understanding of the underlying dynamics and to characterise the process further we have studied the set of distribution functions $\{P(\boldsymbol{r}, t)\}$. First we consider the average density distribution function. It is convenient to study the function $P_T(l, t)$ of $P_T(l - \langle l\rangle, t)$ for the topological bias and $P_E(|\boldsymbol{r} - \langle \boldsymbol{r}\rangle|, t)$ for the Euclidean bias. Here $P_T(l, t)$ is the average probability to find the random walker at a site in chemical distance l from the origin. $P_E(\rho, t)$ is the average probability to find the walker at distance $\rho \equiv |\boldsymbol{r} - \langle \boldsymbol{r}\rangle|$ from the average position $\langle \boldsymbol{r}\rangle$. The simplest scaling ansatz for P_T is

$$P_T(l, t) = \langle l(t)\rangle^{-1} f(l/\langle l(t)\rangle) \tag{4a}$$

and similarly

$$P_E(\rho, t) = \langle \rho(t)\rangle^{-1} g(\rho/\langle \rho(t)\rangle). \tag{4b}$$

The prefactors are due to normalisation. In figure 3 we have plotted $P_T(l, t)\langle l(t)\rangle$ against $l/\langle l(t)\rangle$ and $P_E(\rho, t)\langle \rho(t)\rangle$ against $\rho/\langle \rho(t)\rangle$, both for the bias field $E = 0.2$. The data collapse supports the scaling ansatz of (4). This indicates that essentially one exponent is enough to characterise the *mean* density distributions. It follows from (4) that the corresponding moments $\langle l^n\rangle$ and $\langle \rho^n\rangle$ scale as

$$\langle l^n\rangle \sim \langle l(t)\rangle^n \tag{5a}$$

and

$$\langle \rho^n\rangle \sim \langle \rho(t)\rangle^n. \tag{5b}$$

Next we consider the moments

$$Z(q, t) = \left\langle \sum_{r\in\Gamma} P^q(\boldsymbol{r}, t) \right\rangle \sim L^{-\tau(q)} \tag{6}$$

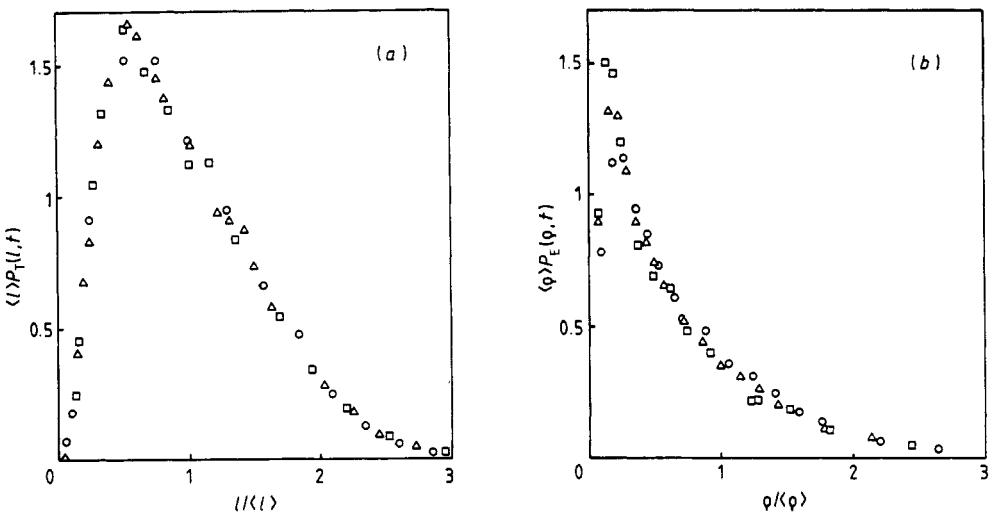

Figure 3. (*a*) Plot of $\langle l(t)\rangle P_T(l,t)$ against $l/\langle l(t)\rangle$ for l between 10 and 170 and for topological bias field $E=0.2$. (*b*) Plot of $\langle\rho(t)\rangle P_E(\rho,t)$ against $\rho/\langle\rho(t)\rangle$ for ρ between 10 and 100 and for Euclidean bias field $E=0.2$. In (*a*) and (*b*) $t=1000$ (○), 2000 (△), and 4000 (□) and averages were made over 400 configurations.

where Γ defines the range $|r-\bar{r}|\leqslant(\overline{r^2})^{1/2}$ for the Euclidean bias and the range within chemical distance $\bar{l}$ from the origin for the topological bias. The bars represent averages over the considered (single) configurational averaged length scale. For the topological bias we have $L\equiv\langle l(t)\rangle$, while for the Euclidean bias $L\equiv\langle x(t)\rangle$ or $\langle y(t)\rangle$. For $E=0$ we choose $L\equiv\langle r^2\rangle^{1/2}$.

Equation (6) defines the set of exponents $\tau(q)$. A similar ansatz has been used, e.g., in studies of chaotic dynamical systems [19], kinetic aggregation [21] or transport in random fields [24].

Defining the number of sites $n(p)\mathrm{d}\ln p$ for which $\ln p$ is in the range $(\ln p, \ln p+\mathrm{d}\ln p)$ we can rewrite (6) as

$$Z(q)=\int p^q n(p)\,\mathrm{d}\ln p \tag{7}$$

where now p stands for $P(\boldsymbol{r},t)$. To obtain $n(p)$ and $Z(q)$ for percolation systems at criticality we have calculated $P(\boldsymbol{r},t)$ for each configuration by the exact enumeration method. This way we have determined the configurational average $Z(q,t)$ and the histogram $n(p)$. In figure 4 we present the histogram $n(p)$ for three cases, zero bias field (broken curve), Euclidean bias ($E=0.2$) (full curve) and topological bias ($E=0.5$) (chain curve). In the presence of the bias fields $n(p)$ shows a broad maximum followed by a long tail which extends to extremely small values of $P(\boldsymbol{r},t)$ at the coldest sites (within the range Γ) of the cluster. This form of $n(p)$ resembles the shape of the growth site probability distribution in kinetic aggregation [21, 22] and the voltage distribution in random resistor networks [23]. In fact, there is a close analogy between these systems and the problem of biased diffusion in percolation systems. In DLA, for example, the growth-site probability distribution p_i is analogous to the function $P(\boldsymbol{r},t)$ discussed here. In DLA the tips of the cluster can be occupied more easily and hence p_i of the tips is large ('hot tips'). On the other hand, only very few particles can get deep inside the fjords and p_i is extremely small there. The hot tips and fjords in DLA

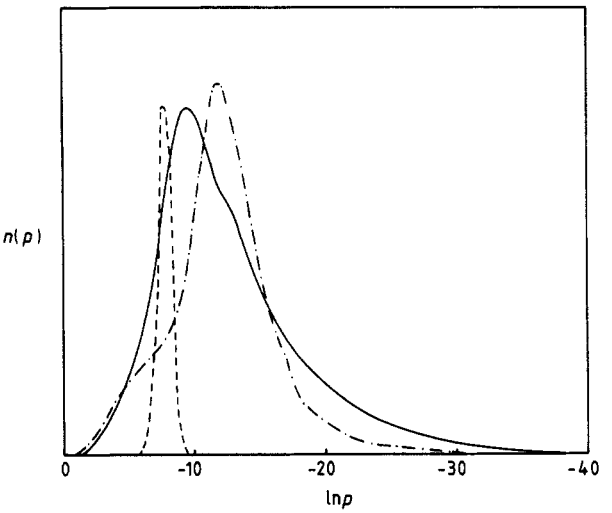

Figure 4. The histogram $n(p)$ of $p = P(r, t)$ with arbitrary units; for zero field, $t = 15\,000$ (broken curve), for Euclidean bias field $E = 0.2$, $t = 4000$ (full curve) and for topological bias field $E = 0.5$, $t = 4000$ (chain curve).

correspond to the hot and cold sites in the biased diffusion problem considered here. The voltage drops play a similar role across the bonds in random resistor networks.

The situation is different without bias field, (figure 4, broken curve). In this case the histogram $n(p)$ is very narrow and a characteristic long tail is completely absent. From kinetic aggregation, for example, we know that a broad distribution $n(p)$ gives rise to multifractal characteristics of the moments $Z(q)$. Therefore the moments cannot be described by a single gap exponent but require an infinite hierarchy of exponents. Thus our findings for $n(p)$ may indicate that for $E > 0$ multifractal features characterise the dynamical process, while for $E = 0$ the moments $Z(q)$ are described by a single exponent. To study this point further we have calculated the configurational average of $Z(q)$ for fixed time t (in the asymptotic regime) and deduced $\tau(q)$ from (6). Results for $\tau(q)$ for several values of Euclidean bias fields are shown in figure 5 and compared with the zero field case. The figure suggests that the whole hierarchy of exponents changes continuously with the field strength E. In the limit $E \to 0$ we find that $\tau(q)$ is linear in q and is described by†:

$$\tau(q) = d_f(q-1). \tag{8}$$

In the limit $E \to 1$ every hot site (see figure 1) represents a trap from which the walker cannot escape. Hence, after a few time steps we have

$$P(r, t) = \delta_{r,r_0} \qquad E = 1 \tag{9}$$

where r_0 is the coordinate of the trap closest to the origin of the walk. Substituting (9) into (6) yields

$$\tau(q) = \begin{cases} 0 & q \geqslant 0,\ E = 1 \\ -\infty & q < 0,\ E = 1. \end{cases} \tag{10}$$

† The slope of $\tau(q)$ depends on the choice of L. If we choose $L = \langle l \rangle$ instead then $\tau(q) = d_l(q-1)$ where d_l is the topological dimension $d_l \simeq \frac{5}{3}$ in $d = 2$.

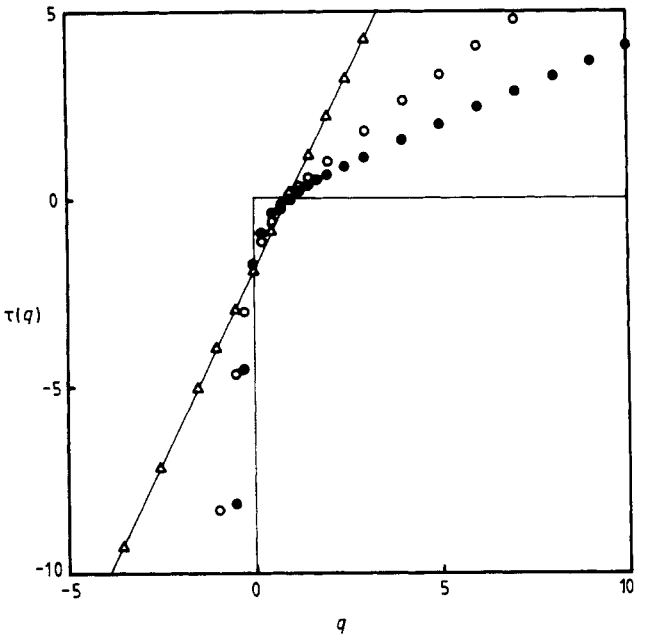

Figure 5. The exponents $\tau(q)$ plotted against q for $E=0$ (△) and several values of the Euclidian bias field $E=0.2$ (○), 0.5 (●), 1.0 (discontinuity at $q=0$ as expressed by equation (10)). The results represent averages over 200 cluster configurations and have been obtained for $t=4000$.

This limiting case is also shown in figure 5. For general E, $\tau(q)$ is a convex function. For large q values, $\tau(q)$ is linear in q, but for small q there is a downward curvature. We obtained qualitatively similar results for the topological bias. It should be noted that for zero bias field our results for $\tau(q)$ converged very well to (8). This supports our conclusion that the multifractal features vanish when the bias field approaches zero. In contrast, for $E>0$ the exponents $\tau(q)$ changed slightly with time. For $q<0$ and $q>1$, $\tau(q)$ tended to decrease with time, while in the interval $0<q<1$ $\tau(q)$ showed a tendency to increase. This tendency excludes the possibility that a simple gap exponent is sufficient to characterise the moments, i.e. that $\tau(q)$ is a simple straight line. It also excludes the case that $\tau(q)$ consists of two straight lines being described by two exponents.

Qualitatively similar results have been obtained for the topological bias.

We thank D Stauffer for critical reading of the manuscript and we gratefully acknowledge financial support from Deutsche Forschungsgemeinschaft, from Minerva, and from the USA-Israel Binational Science Foundation.

References

[1] Böttger H and Bryksin V V 1980 *Phil. Mag.* B **42** 297
[2] van Lien N and Shklovskii B I 1981 *Solid State Commun.* **38** 99
[3] Barma M and Dhar D 1983 *J. Phys. C: Solid State Phys.* **16** 1451
[4] Dhar D 1984 *J. Phys. A: Math. Gen.* **17** L257

[5] White S R and Barma M 1984 *J. Phys. A: Math. Gen.* **17** 2995
[6] Ohtsuki T and Keyes T 1984 *Phys. Rev. Lett.* **52** 1177
[7] Seifert E and Süssenbach M 1984 *J. Phys. A: Math. Gen.* **17** L703
[8] Gefen Y and Goldhirsch I 1985 *J. Phys. A: Math. Gen.* **18** L1037
[9] Pandey R B 1984 *Phys. Rev.* B **30** 489
[10] Stauffer D 1985 *J. Phys. A: Math. Gen.* **18** 1827
[11] Bunde A, Havlin S, Stanley H E, Trus B and Weiss H G 1986 *Phys. Rev.* B **34** 8129
[12] Havlin S, Bunde A, Glaser Y and Stanley H E 1986 *Phys. Rev.* A **34** 3492
[13] Havlin S, Bunde A, Stanley H E and Movshovitz D 1986 *J. Phys. A: Math. Gen.* **19** L693
[14] Stauffer D 1985 *Introduction to Percolation Theory* (London: Taylor and Francis)
[15] Havlin S, Bunde A and Kiefer J 1986 *J. Phys. A: Math. Gen.* **19** L419
[16] Havlin S and Ben-Avraham D 1987 *Adv. Phys.* to be published
[17] Mandelbrot B B 1974 *J. Fluid Mech.* **62** 331
[18] Hentschel H G E and Procaccia I 1983 *Physica* **8D** 435
[19] Halsey T C, Jensen M H, Kadanoff L P, Procaccia I and Shraiman B I 1986 *Phys. Rev.* A **33** 1441
[20] Halsey T C, Meakin P and Procaccia I 1986 *Phys. Rev. Lett.* **56** 854
[21] Amitrano C, Coniglio A and di Liberto F 1986 *Phys. Rev. Lett.* **57** 1016
[22] Nittmann J, Stanley H E, Touboul E and Daccord G 1987 *Phys. Rev. Lett.* **58** 619
[23] de Arcangelis L, Redner S and Coniglio A 1985 *Phys. Rev.* B **31** 4725; 1986 *Phys. Rev.* B **34** 4656
[24] Roman H E, Bunde A and Havlin S *Preprint*
[25] Havlin S and Nossal R 1984 *J. Phys. A: Math. Gen.* **17** L427